Characterization of the SELPO-M polarized electron source on a 100 kV platform

J. Arianer, J. Arvieux, K. Aulenbacher, J. Baudet, N. Duc, S. Essabaa, R. Frascaria, R. Gacougnolle, H.J. Kreidel, R. Kunne, et al.

IPNO-DRE 99.09

Characterization of the SELPO-M polarized electron source on a 100 kV platform

****

Characterization of the SELPO-M polarized electron source on a 100 kV platform

J. Arianer [a], J. Arvieux [a], K. Aulenbacher [b], J. Baudet [a], N. Duc [a], S. Essabaa [a], R. Frascaria [a,1], R. Gacougnolle [a], H.J. Kreidel [b], R. Kunne [a], M. Morlet [a] and G. Roger. [a]

[a] *Institut de Physique Nucléaire CNRS-IN2P3, F91406 Orsay Cedex France*

[b] *Institut für Kernphysik-J. Gutenberg Universität, D-55099 Mainz Germany*

Abstract

A source of polarized electrons based on a helium flowing afterglow has been developed at Orsay. This source, SELPO-M, has been placed on a 100kV platform and set up in such a way as to allow its connection to the MAMI accelerator. Its performances in term of current, polarization and optical properties are given. Its figure of merit ($IP^2 \simeq 75\mu A$) appears highly competitive as compared to strained GaAs sources.

1 Introduction

Spin observables in electron or photon induced experiments are of great importance as can be seen from the experimental programmes in progress or planned at various laboratories like HERA, GRAAL, MAMI, TJLAB, etc... Polarized electron sources with high figures of merit (FOM) are therefore strongly requested. For instance, a parity violation (PV) experiment planned at MAMI and designed to determine the strange form factors of the nucleon requires a high current ($I \geq 25$ μA), high polarization ($P \geq 70\%$) electron beam with good stability and reproducibility over long running periods. To achieve this goal, new technologies have been put in practice at the Orsay Nuclear Physics Institute. The Orsay polarized electron source (SELPO) based on a flowing ^{4}He afterglow optically pumped by a LNA laser, followed by a chemi-ionization between aligned ^{4}He 2^3S_1 atoms and CO_2 molecules, has been able to deliver high currents with high polarization (the FOM was $IP^2 = 40$ μA [1]). Beam

[1] E-mail: frascari@ipno.in2p3.fr

emittance measurements at low current (60% of the total current) and low accelerating potential (200 eV) yielded a normalized emittance of 0.5π mm.mrad, containing 80% of the intensity with a non Gaussian beam profile, and demonstrating the very good quality of this source [2]. To permit the coupling to an accelerator, the source had to be installed on a 100 kV platform with computer controls. Such a development has been made in Orsay in the last two years. This paper describes the source on its platform, designed specifically to inject axially polarized electrons at 100 kV into the injector-LINAC of the Mainz microtron. The different characterization studies are described: emittance, ^{4}He metastable polarization, electron current and polarization, stability and helicity reversal fluctuations. Conclusions about the potential of such a polarized electron source for CW electron accelerators are drawn.

2 SELPO on its platform

The present method that is used to produce polarized electrons has been studied since 1971 by a group from Rice University [3]. The principle of the source is based on the Penning ionization involving optically aligned $He(2^3S_1)$ metastable atoms and singlet ground state CO_2 molecules:

$$He(2^3S_1)\uparrow\uparrow + CO_2\downarrow\uparrow \longrightarrow He(1^1S_0)\downarrow\uparrow + CO_2^+\uparrow + e^-\uparrow$$

The electrons generated are then polarized and extracted through an electrode with a drilled hole called nose. Metastable atoms are created in helium afterglow by means of a microwave discharge cavity operating at 2.45 GHz. The triplet metastable atoms are optically pumped via the D_0 resonant transition [4] by the simultaneous absorption of circularly σ and linearly π polarized light at 1.083 μm (Fig. 1). The optical pumping is produced by a

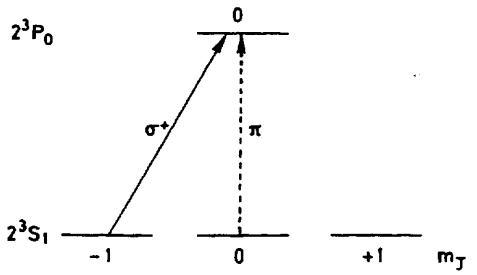

Fig. 1. Helium optical pumping via D_0 transitions.

LNA-laser consisting of a 100 mm long LNA crystal of chemical composition $La_{0.85}$ $Nd_{0.15}$ $MgAl_{11}$ O_{19} which is transversally pumped by Kr-arc lamps in commercial Nd:YAG laser heads [5].

Since April 97, the whole source has been placed on a high voltage platform able to deliver a beam at 100 keV. Its overall dimensions are : L=3.23 m, l=2 m and h=4.4 m. The height is adapted to a beam line level of 3.5 m, given by a necessary height difference with respect to the height of the injector beam line at the Mainz Microtron (1.8 m). The general set up is shown on fig 2. The

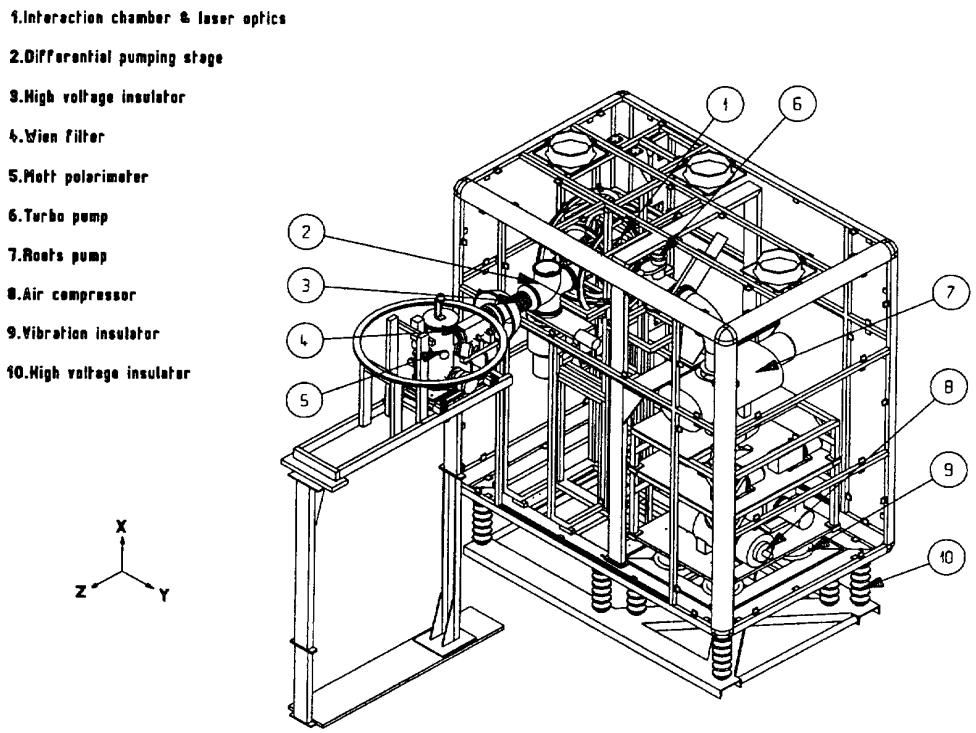

Fig. 2. General arrangement of the source on its platform

electrical power is supplied by a 25 kVA, 100 kV insulating transformer. To avoid beam instabilities, the pumps are supported by an anti-vibrating frame decoupled from the main one. The vacuum system is fully computer controlled. Eleven important source parameters (the voltages of the nose, steerers, and focal lens and the He flux) can be adjusted from the ground potential through optical links . The laser is placed at ground potential and the light is transferred to the source via a 35 m long optical fiber. The σ light is injected on the quantization axis defined by the main magnetic field B_z. This field is collinear to the electron beam momentum, so that the spin direction is longitudinal. After one hour of warm up, the laser can operate for hours in stable condition without any more adjustments.

Some important improvements have been made or tested to enhance the routine performances of the source. The He jet is now produced by a series of 10x0.2 mm diameter glass capillaries to get a more directional flow. This arrangement, commonly used in polarized proton sources, lowers the metastable atom losses onto the walls. The extraction voltage has been increased from 0.6

to 3.5 kV. The total current has been increased by a factor of one hundred at low He pressure. The source normally operates with a LN_2 cooled He purifier with an open circuit. To lower the running costs, we have succesfully tested a closed He circuit, curing the CO_2 pollution and maintaining the 99.9999% purity required to get the nominal metastable atom production.

The source has been placed in a pit for safety reasons. Due to historical reasons (building of a cyclotron with supraconductive coils in the same pit) the stray magnetic field in the pit is 3 G. The region of the optical pumping is surrounded by six coils placed on the three main axis that cancel the stray field components (B_x, B_y) and produces the main magnetic field B_z. An additional coil has been placed on the beam line and oriented in such a way as to cancel the parasitic field at the polarimeter location.

The source has run for more than 2000 hours without any major troubles. Day after day, it starts within a few minutes without readjustment of the previous set of parameters. A 14 mA total polarized e-beam is collected on the 10 mm diameter nose, at a He pressure of 1.2 10^{-1} mbar compatible with a full atomic polarization. It is then possible to extract a beam of up to 1 mA through a 2 mm diameter hole which faces the chemi-ionization region.

The stray field of 3 G within the pit where the source has been placed has been somewhat problematic especialy for the diagnostics inside the polarimeter. A shielding of the accelerating gap has been installed temporarily to increase the transmission for emittance measurements. At high extracted intensities, (beyond some μA), it is necessary to scrape the beam through three successive 1 mm diameter defining holes along the beam line, to lower the beam current down to some nA on the target. This collimation unfortunately generates parasitic X-ray fluxes hindering the polarization measurements. A special lead shielding surrounding the detectors in the polarimeter and the polarimeter itself has been installed to obtain cleaner spectra.

3 $^4He(2^3S_1)$ metastable atom spin polarization

3.1 Experimental setup

The electron polarization performance depends critically on the achieved atomic polarization. A qualitative indication on the efficiency of the optical pumping is obtained by measuring the $He(2^3S_1)$ spin-state populations. The technique used to determine these quantities is described in detail in reference [6]. The principle consists in measuring the absorption by the metastable atoms of a weak probe beam light propagating through the afterglow using a compact

optical system. The purpose of these measurements is not to make an exhaustive study of the atomic polarization, but to check the good operation of the optical pumping in the afterglow.

The probe beam propagates along the main magnetic field axis. It is generated by a 50 mW laser diode. The linear polarization of the light is transformed into circular polarization by means of a quarter wave plate continuously rotating at a frequency $\omega \simeq 17$ Hz. The light is emerging at a small angle with the B_z field ($\simeq 10°$). Since the beam absorption is low, a metallic mirror is used to reflect the transmitted light back through the chamber, then the ratio noise/signal is minimized. The transmission of the beam is measured at the same angle by a photodiode. The absorption signal is synchronously detected at twice the rotation frequency of the $\lambda/4$ plate using a lock-in amplifier. The laser diode has a single-mode operation with an estimated width of 3 MHz. The laser frequency is tuned on the D_0 ($2^3S_1 \rightarrow 2^3P_0$) resonance transition of the helium. The tuning is performed by controlling the diode temperature.

3.2 Results and discussion

Typical measured values of polarization as a function of the laser intensity are displayed in Figure 3. The measurements are done in routine working

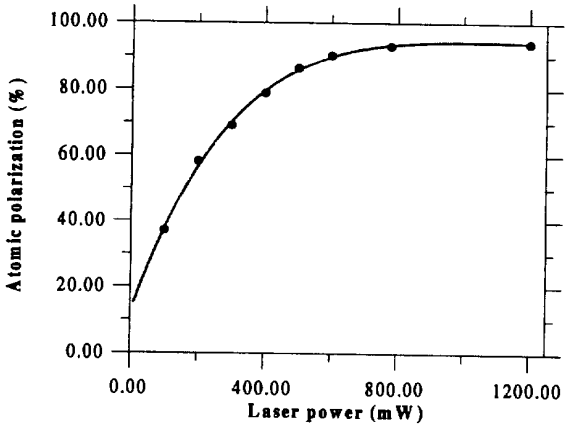

Fig. 3. The atomic polarization as a function of the laser power available in σ or π pumping channel.

conditions for the source : the operating pressure of the helium is limited to 0.09 mbar in the afterglow and the CO_2 flux is about 70 cm^3s^{-1} STP. The extracted current from the source at this pressure is more than 150 μA. The recorded polarization data saturate at 94%: this value is reached asymptotically for a useful laser intensity of 1200 mW. The figure shows that a laser intensity of 600 mW per pumping channel (σ and π) is enough to saturate

almost completely the polarization. The imperfections of the quarter-wave plate as well as the defects of the detection electronics have to be considered. The uncertainty is estimated to be approximately 4%. A similar behavior has been observed in data obtained at pressures lower than 0.09 mbar [6]. As the pumping beam is not completely homogeneous, the polarization is spatially dependent. Therefore, the present measurement procedure gives an average polarization of the 2^3S_1 atoms illuminated by the probe beam.

The polarization, measured with the σ beam light alone, is between 47% and 49%. The measured ratio $P_\sigma/P_{\sigma+\pi}$ of the σ polarization to the total polarization is about 1.96, which is consistent with the theoretical value of 2, when the σ polarization saturates at 50%.

Measurements have been done to analyze the effect of the components of the stray field ($\simeq$3 G) within the pit. The data are given in table 1. In this table, the indicated magnetic field components are those given in the optical pumping region. The data indicate that a B_z field component of 3 G into the reactant

Table 1
Stray field effect on atomic polarization.

B applied (G)			P (%)
B_x	B_y	B_z	
1.6	2.7	5	90
1.6	2.7	3	90
1.6	2.7	1	70
0	2.7	3	59
1.6	0	3	70

chamber is necessary to obtain an efficient optical pumping. The correction on the two other components have been optimized to avoid any degradation of the atomic polarization.

3.3 Emittance measurements

The hardware and software used for this measurements were exact copies of the instruments used at the Mainz Microtron. Therefore the results can be directly compared to the required parameters at Mainz. The measurements have been done with a wire scanner separated from a solenoid by a drift space of 0.5 m. The method employed for emittance determination is the measurement of the beam width under different focussing conditions. [7,8] Beam diameter is determined by taking $\pm 2\sigma$ of the measured charge distribution, this means

95.4% of the beam current will be included, if a gaussian distribution is assumed.

Measurements were done at a beam energy of 30 keV because of the necessity to install additional magnetic shielding in the accelerating gap. The shielding helped optimizing the beam transmission close to 100%, but limited HV-capability. With a further optimized shielding, operation at 100 keV beam energy with good transmission was achieved. However, the shielding changed the focussing properties: Emittance measurements were not possible because this would have required to have matching lenses and drift space before the emittance measuring section. This space was not available under the restrictions of the set-up in the pit.

The results for vertical and horizontal emittance are presented in Fig. 4, the normalized values can be obtained from the measured values by applying: $\epsilon(norm) = \beta \cdot \gamma \cdot \epsilon(30keV)$. This results in a normalized value of 1.3π mm.mrad, which is considerably larger than the one which was determined at lower energy with a different method. [1] A direct comparison is difficult because of

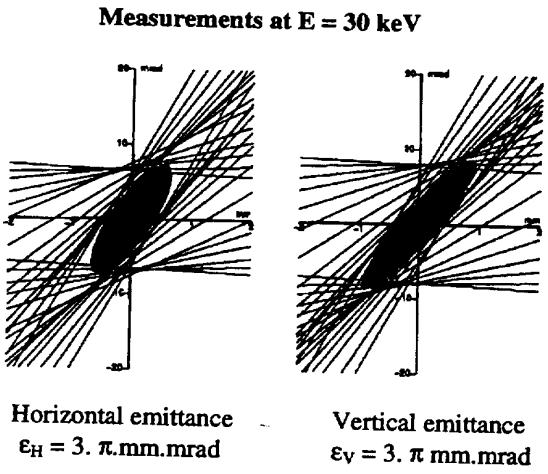

Fig. 4. Emittance diagrams

the different experimental methods applied, see e.g. [9]. However the observed difference can be explained as a result of our method determining beam width, which delivers another emittance value compared to methods like rms ($\pm 1\sigma$) or FWHM (e.g. our emittance value using $\pm 2\sigma$ is 4 times higher than the value obtained if using rms beam width). The results indicates that the inherent emittance of the source did not give the required value of the Mainz microtron of 0.65π mm.mrad. This desired value may be achieved by external collimation of the beam behind source. The loss of beam current coming from such a collimation depends on the charge distribution in the beam but should be in any case lower than a factor of two. The current density profile is very peaked. About 50% of the beam flows through the first 1 mm diameter

scraping hole, the surface of which is only 6% of the beam cross section.

The extreme sensitivity of the μ-wave cavity to vibration causes beam instability increased by the large 3 lens magnification (> 25). Presently, the current instability is less than 5% and the position jitter, at the scanner position, is 1 mm for a 5 mm spot beam diameter. The beam intensity and position stabilities need to be improved. Optimization of the extraction geometry can be made as suggested in reference [10]. An improvement in position stability can also be obtained by using systematically an anti-vibrating system. Such a system made of four pneumatic stabilizers has been built but not used in the present measurements.

4 Electron polarization measurements

The polarized electrons freed by chemi-ionization are extracted through a narrow hole in the nose, ranging from .8 to 2 mm in diameter. The electrons

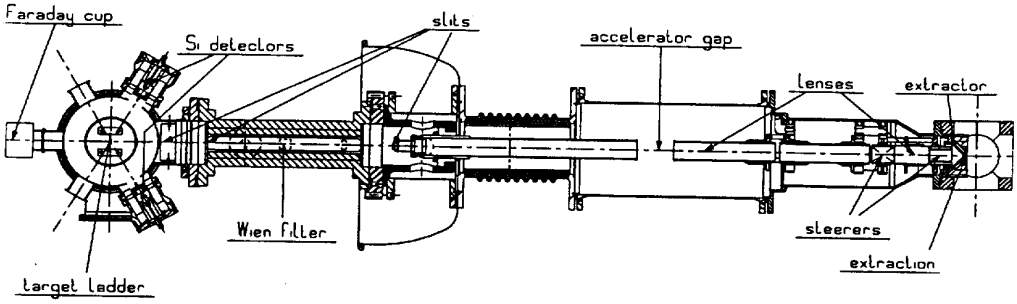

Fig. 5. Electron beam line for electron polarization measurements

are accelerated and focused on a target for polarization measurements. The transport up to the Mott polarimeter is shown in Fig. 5.

4.1 Principle of the measurements

The electron polarization has been measured with a polarimeter using Mott scattering [11] in which a transversally polarized electron beam is scattered by a high-Z nucleus (here a gold foil) producing at large angles a left-right asymmetry, due to the spin-orbit interaction. For energies between 25 and 120 keV, the theoretical analyzing power (or Sherman function) S_{th} for single scattering has a broad maximum between 100° and 140° which is approximately centered around 120° [12]. As an example, at 100 keV, $S_{th} = 0.391$ [13]. However the effective Sherman function, S_{eff}, is smaller due to the effect of multiple (small

angle) and plural (large angle) scattering. The importance of these two effects varies with the incident energy, plural scattering being favored at low energy (below 50 keV) and multiple scattering being dominant at higher energies [14]. Since in a standard (without retarding potential) polarimeter, all scattered electrons are detected, the energy resolution is limited by the detector resolution, which is usually of the order of 10-20 keV for the type of detector (Si detector) used in these measurements. Such a resolution does not allow the separation between elastic and inelastic events. One way to solve this problem, is to do measurements with target foils of different thicknesses and then extrapolate to zero thickness where, by definition, multiple scattering is absent. The difficulty of this procedure is that the smallest finite thickness which can be investigated is of the order of a few nanometers and that large uncertainties affect such an extrapolation, as will be discussed below.

4.2 Polarimeter description

Gold foils with a diameter of 10 mm, and 5, 10, 50 and 100 *nm* thick are mounted on a movable vertical target ladder. Targets with thicknesses 50 *nm* and 100 *nm* are self-supporting. The 5 and 10 *nm* targets are mounted on a support made of a Formvar® foil [composition: 82% ($C_8H_4O_2$) + 12% ($C_3H_6O_2$) + 6% (C_2H_4O)] about 100 *nm* thick. An empty target mounting allows no-target measurements. A full to empty ratio better than 1000:1 is usually observed. A single 100 *nm* thick Formvar® foil is also mounted on the target ladder for subtraction of the support contribution. The counting rate for the support is typically of the order of a few per cent compared to a 10 *nm* Au target. Its asymmetry is essentially zero due to its low Z. Therefore support corrections amount to 2-6 % depending on the gold target thickness. The comparison between the counting rates obtained for the 5 and 10 *nm* targets indicates that the true thickness of the 5 *nm* target is more probably close to 6.5±0.5 *nm*.

The detectors, are 100 μm thick surface barriers Si detectors. The applied voltage is 40 V, a compromise between depletion depth and energy resolution. They are connected to charge preamplifiers (CPA). The CPA are followed by linear amplifiers and then by a quad single-channel-analyzer (SCA) which selects the elastic peak and rejects some low energy background. The gated signal is sent to a PC which drives, through a HPC2 interface, the following measurement pattern: measurement with one spin direction, rotation of the quarter-wave ($\lambda/4$) plate (see Section 3.1) reversing the helicity, and a subsequent measurement. A selection of the number of measurements to be averaged (usually 10 per spin state) can be preset.

In order to minimize pile-up effects, the counting rate has been limited to

~500 Hz in the elastic peak (corresponding to currents of the order of a few nA to a fraction of a nA on the target, depending on target thickness), but tests with rates up to 4 kHz have shown no noticeable effects on the measured polarization. Overall statistics is of the order of 10000 counts per measurement or more, yielding a better than 1% FWHM uncertainty on the asymmetry.

Typical resolution of the electronics with pulser is of the order of 15 keV. On fig. 7 one can see that the overall resolution is of the order of 18 keV FWHM. The peak height to background ratio is 9/1 for a 100 *nm* target (see 4.1). The resolution is not as good as some results reported in the litterature. For example, in their review article Gay and Dunning [14] cite resolutions of 10 keV and Fletcher *et al.* [15] show spectra with 13 keV FWHM resolution and a signal-to-background ratio better than 25/1. Some of our difficulties come from a bad electromagnetic environment (the hunt for parasitic oscillations has been painstaking).

Another problem is the fact that the Wien filter is placed immediately before the target chamber without any optical element to clean up the beam. Since the Wien filter is highly defocussing, its necessary operation produces some of the observed background.

A third source of background is the Faraday cup which is very close (12 cm) to the detectors. Displacing it 5 cm downwards and the application of a transverse magnetic field to clean up retroscattered electrons have resulted in mild improvements. The solution to these problems can only come for a better environmement with a beam line having momentum selection (dipoles) and focusing elements (quadrupoles).

The energy of polarized electrons can be varied continuously from 0 to 100 keV, but the Wien filter limits the operation to 80 keV for full 90° spin rotation. For safety reasons most of the measurements have been done at 70 keV with only a few ones made at higher energies. As seen on fig. 6, during the asymmetry

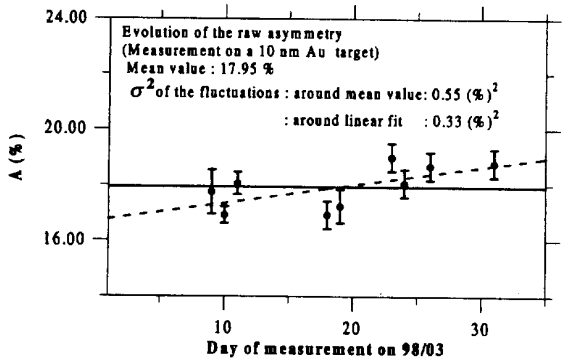

Fig. 6. Relative asymmetries measured at $20\mu A$ as a function of the date of measurements

measurement campaign of March 98, a good stability and reproductibility of the asymmetries has been observed. The small increase of A with time is due to a better control of the different tuning parameters.

4.3 Results

The polarization of the electron beam is related to the measured asymmetry through:

$$P = A/S_{eff}$$

where S_{eff} is the effective Sherman function. In order to deduce the polarization, one must first correct the raw experimental asymmetries for background contributions, then take inelastic scattering into account by extrapolating to zero thickness and finally estimate S_{eff} for that thickness. We address these 3 points in detail in what follows.

4.3.1 Background subtraction

Typical spectra for different target thicknesses are shown in fig. 7. They consist in a flat plateau whose height varies from 7 to 14% of the height of the elastic peak, extending below that peak in a way which is not easy to determine. A possible parabolic shape is shown in fig. 7.

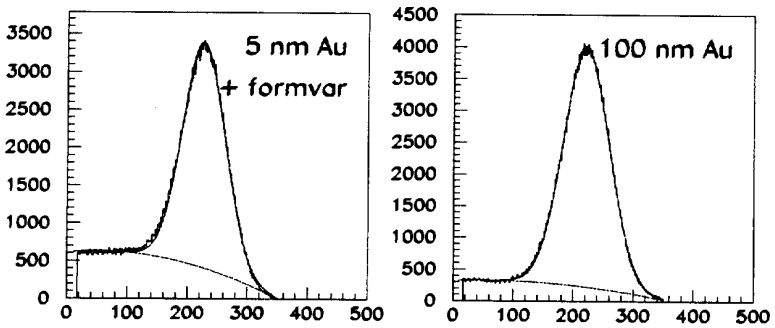

Fig. 7. Energy spectra from a Si detector taken with 70 keV electrons, scattered at 120° on a 5 and 100 *nm* Au targets

This background is not related with the incident beam since it is completely absent when one uses an empty target frame, instead of a Au target. It comes probably from electrons elastically scattered at forward angles (for which the cross-sections are huge) and then back-scattered inelastically by surrounding material (collimators, walls,...). Due to the remnant field of the pit, the spectra of left and right detectors are not identical in shape, despite the correcting

coil. (see Section 2). This comes from the fact that the scattered electrons are not bent symmetrically to the left and to right in a transverse field.

In the present analysis a triangular shape for the background has been used as an approximation for background subtraction to the data [15]. This method yields to slightly smaller asymmetries, but it gives smaller systematic error. The effect of this correction is to multiply the aymmetry by a factor of 1.08±0.01 almost independent of the target thickness, which is another indication that the background is target related.

For the thinner targets, made of Au deposited on a 100 *nm* support, the effect of the support, measured in separate runs, is further subtracted, yielding an increase of the asymmetry by a factor 1.06 for the 6.5 *nm* target and 1.038 for the 10 *nm* target. These values are typical of a standard polarimeter [15].

4.3.2 Extrapolation to zero thickness

The usual procedure to get rid of inelastic effects is to do measurements with decreasing target thicknesses and extrapolate the background corrected asymmetry to zero thickness. A number of functional dependencies can be found in the literature (see the review article of ref. [14] for details), the most appropriate one being [16]:

$$A = a + b^{-t}$$

In figure 8 are shown the following approximations : linear in $1/\sqrt{A}$ (χ^2=1.05

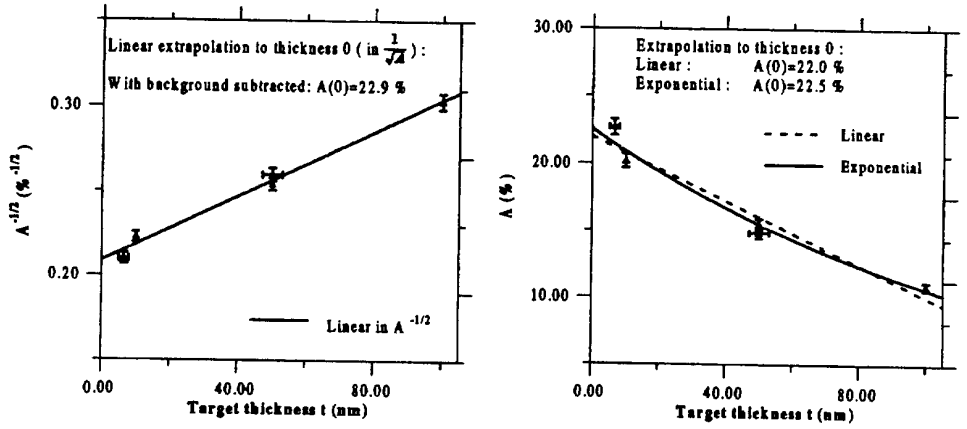

Fig. 8. Experimental asymmetries as a function of the target thickness with the values obtained at 0 by different extrapolation modes.

per degree of freedom), exponential (χ^2=1.89) and linear (χ^2=5.09). The best χ^2 is obtained for the extrapolation linear in $1/\sqrt{A}$. The asymmetry extrapolated to zero thickness is respectively: 22.9%, 22.5% and 22.0%.

After background subtraction, the asymmetry no longer depends on the inelastic events or support effect but only on multiple or plural scattering. This is in agreement with the gaussian shape observed for the peak after background subtraction (fig. 7). The correction factor, $A(0)/A(t)$, to apply to A(t) is given on fig. 9. This correction remains close to a linear function of the

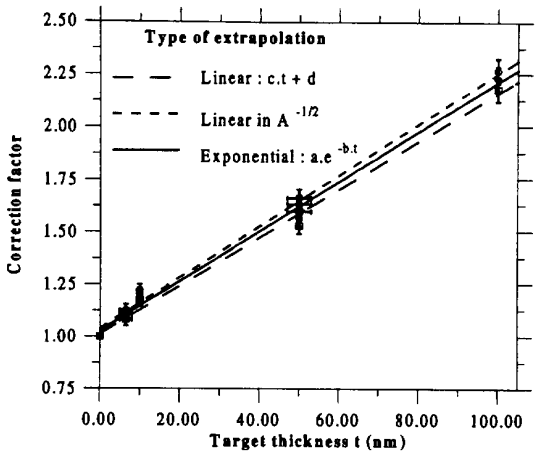

Fig. 9. Correction factor to apply to the asymmetry A(t) after background subtraction. The three points correspond to the 3 types of extrapolation, and the lines are a linear fit for each of those.

target thickness and depends only slowly on the type of extrapolation.

4.3.3 Determination of S_{eff}

The theoretical value calculated at 70 keV for single scattering by one atom is S_{th}=0.373 [12,17]. A rough estimate on the precision of the theoretical calculations is of the order of 1% when comparing results of ref. [12,17].

Due to remaining plural scattering effects, which are not corrected by the background subtraction or extrapolation procedure [14], S_{eff} is smaller than S_{th}, the difference being larger for smaller electron energies. An interpolation of the data obtained until 1989 with retarding potential polarimeters, yields a value $S_{eff} = 0.367 \pm 0.003$, very close to the theoretical value. The uncertainty attached to such a procedure has been estimated to be $\sigma = \pm 5\%$, in a study of a standard polarimeter very similar to the present one but with a slightly better resolution and S/N ratio [15].

Using $S_{eff} = 0.367$, the following beam polarization depending on extrapolation procedure, is obtained:

$1/\sqrt{A}$: P=62.4±3.8% ; exponential: P=61.3±3.8% ; linear: P=60.0±3.8%

The dispersion of the results is an indication of the systematic uncertainty. The adopted value for P is : 61.9±3.8±3.2%.

4.3.4 Polarization dependence with intensity

A study of polarization as function of the extracted electron intensity has been done on the 10 nm thick Au target. In order to limit the intensity on target, the beam has been defocussed in front of the first slit shown in fig. 5. The ratio

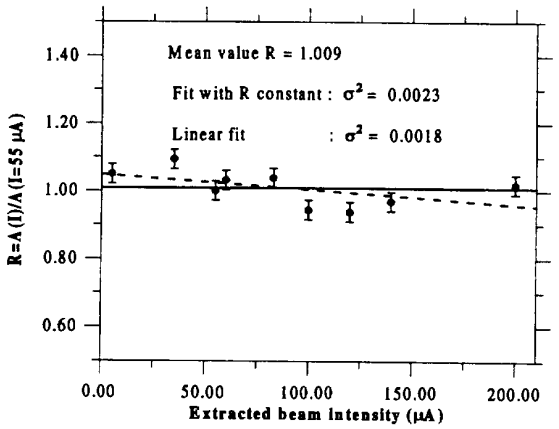

Fig. 10. Asymmetry variation as a function of the extracted electron beam intensity.

between the asymmetry at a given intensity and the asymmetry measured at 55 μA as a function of the extracted beam intensity is given on fig. 10. The reference value has been taken at 55 μA, the measured asymmetry being then close to the mean value over the range of measurements. A fit with a constant is in good agreement with the data. A linear fit with a negative slope does not improve significantly this result.

5 Helicity states mixture

In the parity violation electron-proton elastic scattering experiment foreseen at MAMI, a random helicity reversal at a frequency multiple or submultiple of the parasitic 50 Hz is needed. Therefore, an another important value that characterizes the source is the time necessary to switch from one polarization state to the other. To measure this value the quarter wave plate was replaced by a Pockels cell. A driving voltage of about 5 kV gave the optimal circular polarization.

To adjust the polarization angle with respect to the crystal axis, a linear

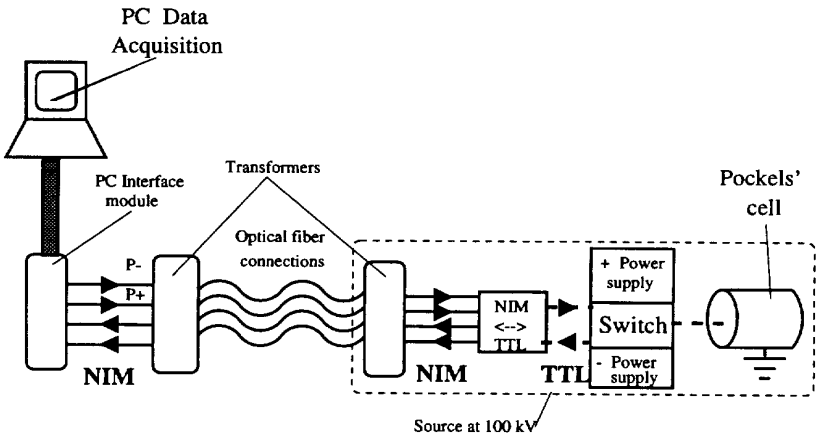

Fig. 11. Schematic view of the switching time measurement set-up

polarization rotator ($\lambda/2$ plate) was placed just before the cell. As the beam was slightly cut by the optical elements for reasons of space and as the crystal coating was not particulary well suited for the wavelength of the laser, the beam transmission through the optical system was 50%. Taking into account the power of the laser this was approximately sufficient to saturate the atomic polarization. For this measurement only σ beam light was used , as it was difficult with this set-up to achieve a good overlap between the σ and π beams.

The set-up used for the switching time measurement is shown in figure 11. A high voltage switch with a switching time of the order of 0.5 ms was used to switch rapidly between the positive and negative voltages, furnished by two FUG HV supplies. The switch was piloted by a pulse generated by a National Instruments PC-TIO-10 card, driven by a Labview application running on a PC. The latter program also ensured the data acquisition. The PC and the

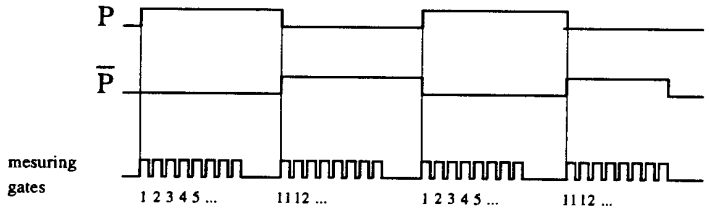

Fig. 12. Polarization and measurement gates

switch were interfaced by a dedicated module that generated the polarization states and the measuring gates. The module also distributed the detector signals to the correct scalers of the PC-TIO-10.

During a measurement the signals of the detectors are sampled at fixed times and durations within each polarization gate (figure 12). The variation of the polarization is calculated by summation of the samples that correspond to the same time-slot and the same polarization and combining them into an

asymmetry.

The main result is shown in figure 13. For this measurement a polarization

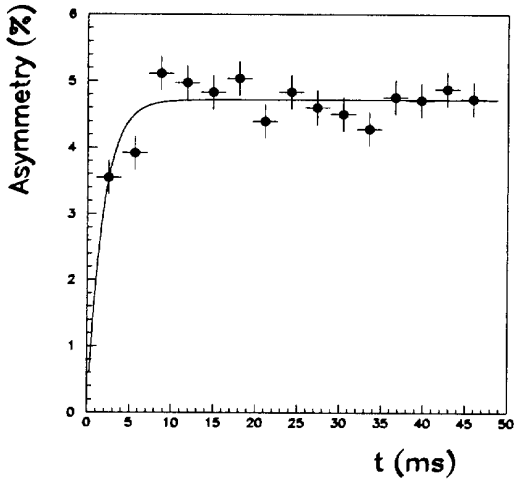

Fig. 13. Result of the switching time measurement. The fifteen measurements within the polarization gate are 3 ms long and fitted to an exponential. Only σ beam light was used for this measurement

gate of 50 ms was used, divided in fifteen 3 ms time–slots. The switching time deduced from the measurement by an exponential fit, was 1.8 ± 0.7 ms.

6 Conclusions

The source SELPO has been successfully installed on a 100 kV platform. A very intense polarized electron beam of more than 10 mA is produced by Penning ionization of an optical pumped ^{4}He metastable afterglow. The atom polarization obtained by $\sigma + \pi$ polarized light pumping reaches 94%. The extracted electron beam through a nose of 2 mm diameter is about 1 mA. To characterize the properties of this electron beam, polarization and emittance measurement have been done. The technique used for the polarization measurements which is based on Mott scattering, needs a special optical beam line defocussing the beam in order to reduce the intensity on target at a few hundred of pA. This method produces a large background and supposes that the polarization is kept the same. The measured asymmetry is A=22.7±1.4±1.2%, which with S_{eff}=0.367±0.003 yields to a polarization P=61.9±3.8±3.2%. The large uncertainty on this result comes mainly from the extrapolation technique at zero target thickness and from the poor energy resolution of the electron detection as compared to the Campbell [13] or Gay [14] polarimeter types previously used [1]. The factor of merit (FOM) of the source is now $IP^2 \simeq 75\mu A$.

The emittance envelope measurement leads to ϵ_N=1.3πmm.mrad for the normalized emittance. With the observation which is made of a very peaked beam spot, one may foresee a beam of about 100 μA in an emittance of ϵ_N=0.5-0.7πmm.mrad after some cuts before acceleration in the first MAMI microtron.

The study of the ability of a fast helicity reversal at about 50 Hz has been done showing that a mixture of the two different spin states no longer subsists after 2 ms, allowing the use of such a kind of source for a parity violation experiment.

Some complementary studies have to be done. They concern mainly the beam instabilities and the search for the origin of the electron polarization loss as compared to the atomic polarization. This needs a cleaner stray field environment with a new beam line having more focussing elements and diagnostics, as proposed in reference [10].

This kind of source seems to be a very promising alternative to AsGa type sources. New developments can be envisaged. The general geometry of the source can be deeply modified. The Roots blower system may be replaced by a compact hybrid turbopump able to work at 0.1 mbar. The metastable atoms may be generated with a hollow cathode or with a transverse linear gun to avoid ionization electrons. The He flow may be launched with a supersonic jet generator. The optical pumping may be operated by a set of laser diodes or by a fiber laser. With these improvements, it would possible to fit the source in a volume smaller than 1 m^3.

Acknowledgements

The authors are greatly indebted to F. B. Dunning, K. G. Walters and G. H. Rutherford for their help in the conceptual design of the source, to M. Leduc and C. G. Aminoff for the LNA laser and to J. Hamel for the probe laser. Many thanks to A. Mueller for interesting comments and discussions. The IPN staff is greatly acknowledged for his support during different phases of the characterization of the source, particularly M. Arianer, P. Dubois, M. Kaminsky, R. Margaria and R. Skowron.

References

[1] J. Arianer et al., **Nucl. Inst. and Meth. A 382** (1997)371.

[2] S. Cohen et al., **J.of Phys. D**: Applied Physics, **30**(1997)417.

[3] M. V. Mc Cusker, L. L. Hatfield and G. K. Walters **Phys. Rev. A 5**(1972)177.

[4] L. D. Schearer and Padetha-Tin, **J. Appl. Phys. 68**(1990)943.

[5] C. G. Aminoff, C. Larat, M. Leduc and F. Laloe, **Rev. Phys. Appl. 24**(1989)827.

[6] S. Essabaa et al. **Nucl. Inst. and Meth. A 344** (1994)315.

[7] H. Aufhaus, **PhD-thesis**, Institut für Kernphysik, Uni-Mainz (1981).

[8] H.-J. Kreidel, **PhD-thesis**, Institut für Kernphysik, Uni-Mainz (1987).

[9] C. Lejeune and J. Aubert: Appl. charge particle optics, Adv. in electronics and electron physics , **E. Septier (ed.) 13A**(1980)159.

[10] S. Cohen. Orsay, Internal report **SELPO 97-01** (1997).

[11] N.F. Mott, **Proc. R. Soc. A 135**(1932)429.

[12] G. Holzwarth and H.J. Meister, **Nucl. Phys. 59** (1964)56.

[13] D.M. Campbell, C. Hermann, G. Lampel and R. Owen, **J.Phys.E: Sci. Instrum. 18**(1985)664.

[14] T.J. Gay and F.B. Dunning, **Rev.Sci.Instrum. 63** (1992)1635.

[15] G.D. Fletcher, T.J. Gay and M.S. Lubell, **Phys. Rev. A34**(1986)911.

[16] T.J. Gay et al., **Rev.Sci.Instrum. 63**(1992)114.

[17] A.W. Ross and M. Fink, **Phys. Rev. A38**(1988)6055.